

Supporting information

NSTAR characteristics

Table S1. Main characteristics of the commercial nZVI (NSTAR) used in the synthesis of NCs [47]. SSA corresponds to the specific surface area.

nZVI	Presentation	Composition	Size (nm)	SSA (m ² g ⁻¹)
NSTAR	powder	Fe(0) ≥ 65-80% Fe ₃ O ₄ ≤ 20-35%	50-65	20-25

Dynamic Mechanical Analysis detailed procedure and fundamentals

Figure S1 shows the experimental arrangement used for the measurement.

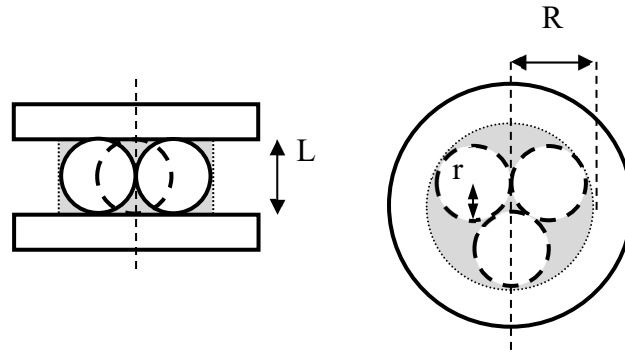


Figure S1. Experimental arrangement used for DMA. a) side view, b) top view.

To calculate stress applied to this configuration of spheres, it is assumed that they form a cylinder of length $L = 2r$ and a radius R , whose projection is denoted in the shaded area. The radius R of the cylinder, which is given by Descartes' circle theorem [1], establishes the relationship between four circles tangent to each other through their curvature k :

$$k_1 + k_2 + k_3 + k_4 = 2(k_1^2 + k_2^2 + k_3^2 + k_4^2) \quad (1)$$

$$k_i = \pm 1/r_i \quad (2)$$

In our configuration:

$$k_r = \pm 1/r \quad (3)$$

$$k_R = \pm 1/R \quad (4)$$

$$k_R = (3 \pm 2\sqrt{3})k_r \quad (5)$$

Of the solutions obtained, the one that corresponds to the desired circle is:

$$R = 2.155 r \quad (6)$$

Because the dimensions of the spheres are similar in all cases, to comparatively analyze the different formulations it can be assumed that the assumption made in the geometry of the sample

I. Rychluk et al. Harnessing chitosan beads as an immobilization matrix for nZVI for the treatment of Cr(VI) contaminated laboratory residue.

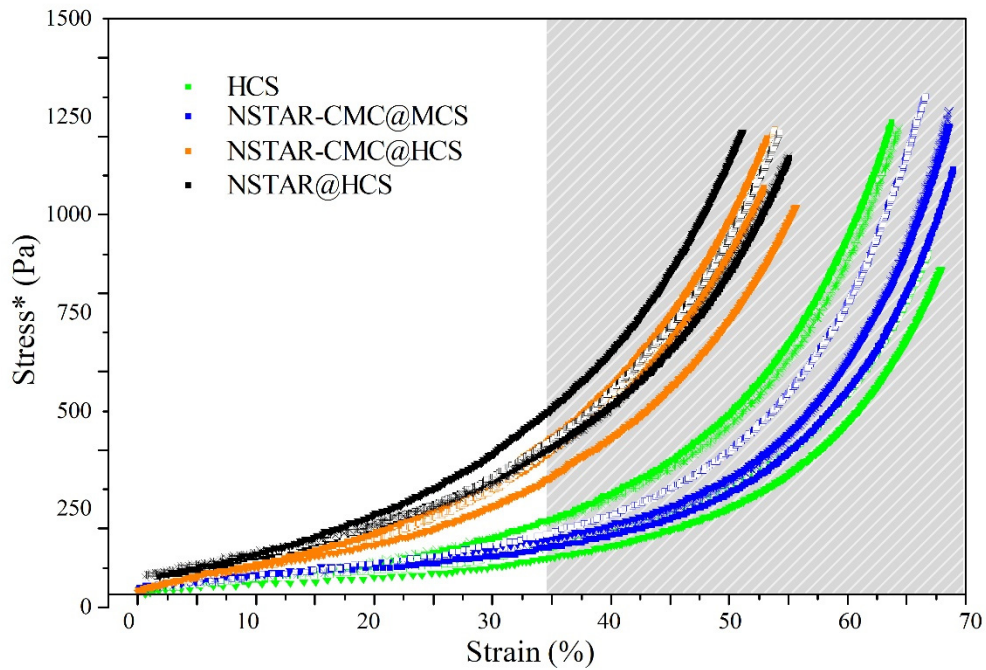
will not affect their tendency, but in the results the value of stress will be reported as Stress*, calculated from the force signal applied by the equipment:

$$\text{Stress}^* = \text{force} / \pi R^2 \quad (7)$$

Stress*-strain curves obtained show a significant dispersion for the same sample, typical of systems of this type, and even using the lowest rate of force increase offered by the equipment, the moment in which the spheres collapse cannot be determined. It is observed that at high strains, all samples produce the same curvature, indicating that the contribution of the lower plate material is dominant, which invalidates this part of the tests (between 30 and 60% strain).

However, at any strain level, it is observed that the stress*-strain curves are grouped into 2 well-defined sets: the curves obtained for the NSTAR@HCS and NSTAR-CMC@HCS samples indicate greater initial stiffness (and less dispersion in data) with respect to the HCS and NSTAR-CMC@MCS samples.

(a)



I. Rychluk et al. Harnessing chitosan beads as an immobilization matrix for nZVI for the treatment of Cr(VI) contaminated laboratory residue.

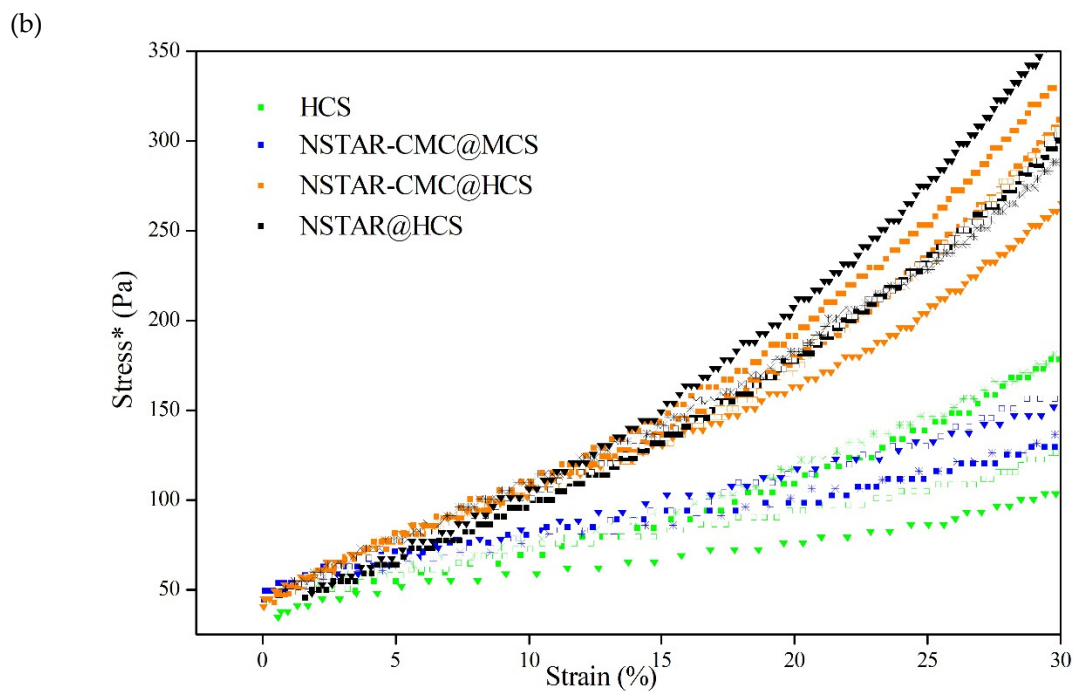
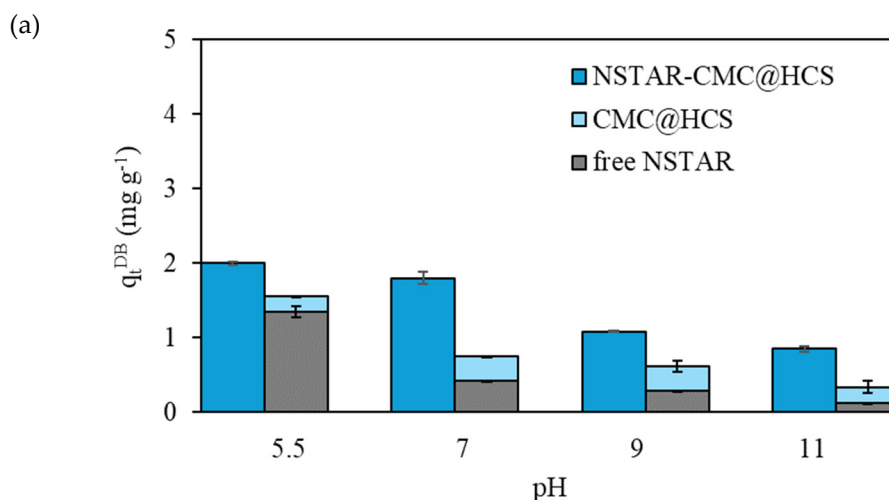


Figure S2. Stress*-strain obtained from the DMA for, NSTAR@HCS, NSTAR-CMC@MCS, HCS and NSTAR-CMC@HCS. a) up to 60% strain, b) up to 30% strain.

This indicates that at low stresses as expected (or desired) in the operation, at the same stress level the spheres of the first group will deform less and will tend to collapse less than the spheres of the second group.

Removal of Cr(VI) in Synthetic Aqueous Solutions: pH and Immobilization of the nZVI as Variables



I. Rychluk et al. Harnessing chitosan beads as an immobilization matrix for nZVI for the treatment of Cr(VI) contaminated laboratory residue.

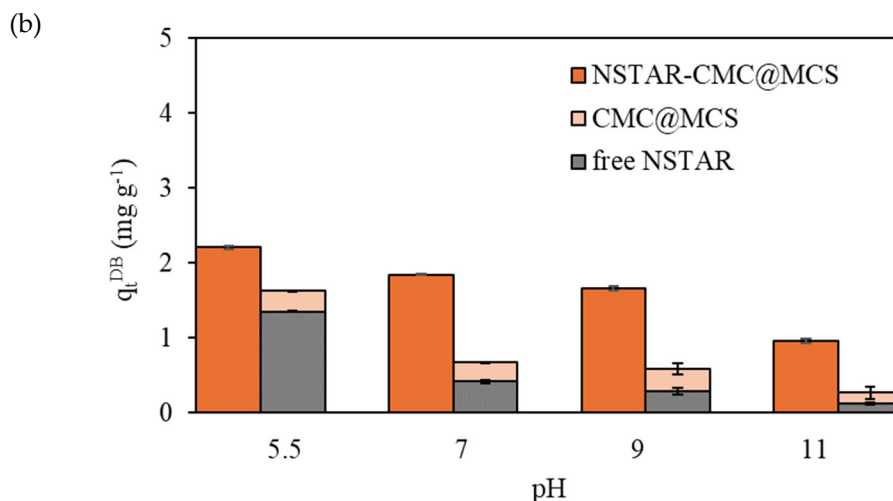
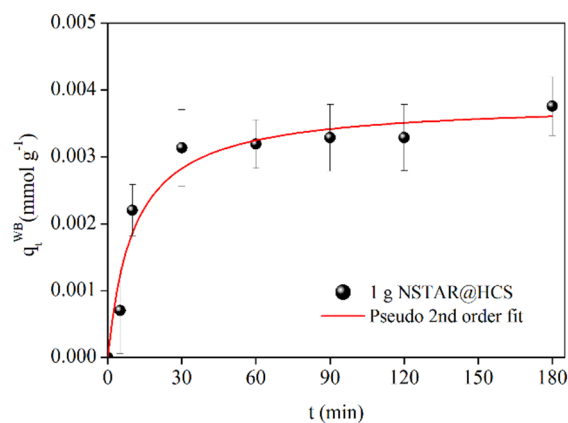


Figure S3. Cr(VI) q_t^{DB} removal capacity obtained for (a) NSTAR-CMC@HCS, CMC@HCS, and free NSTARs in solution, (b) NSTAR-CMC@MCS, CMC@MCS, and free NSTARs in solution. Initial conditions: Synthetic water, $[\text{Cr(VI)}]_0 = 65 \mu\text{M}$, 0.7 g NCs, pHs: 5.5, 7, 9 and 11.

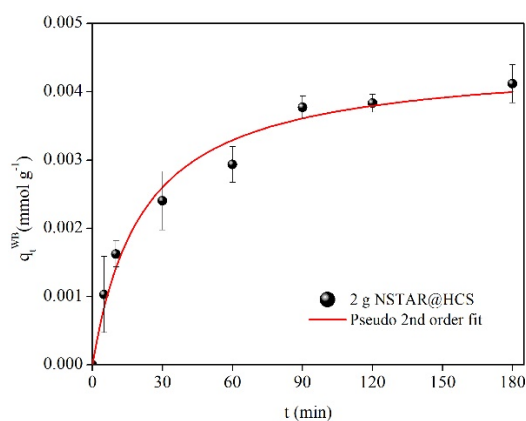
Real Water Removal Kinetics with Cr(VI)

Figures S4 (a) to (e) show the kinetic adjustments for each Cr(VI) removal experiment, incorporating 1 to 6 g of NSTAR@HCS in each case.

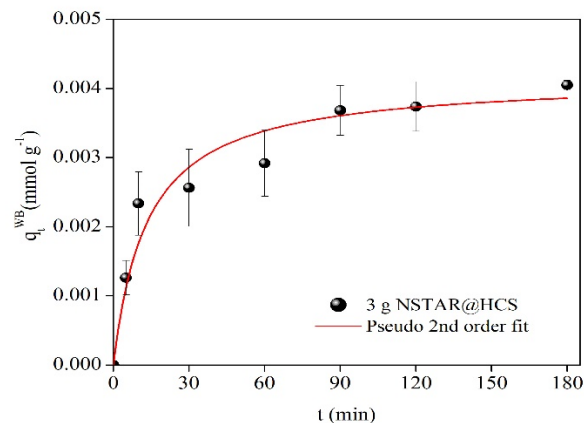
(a)



(b)



(c)



I. Rychluk et al. Harnessing chitosan beads as an immobilization matrix for nZVI for the treatment of Cr(VI) contaminated laboratory residue.

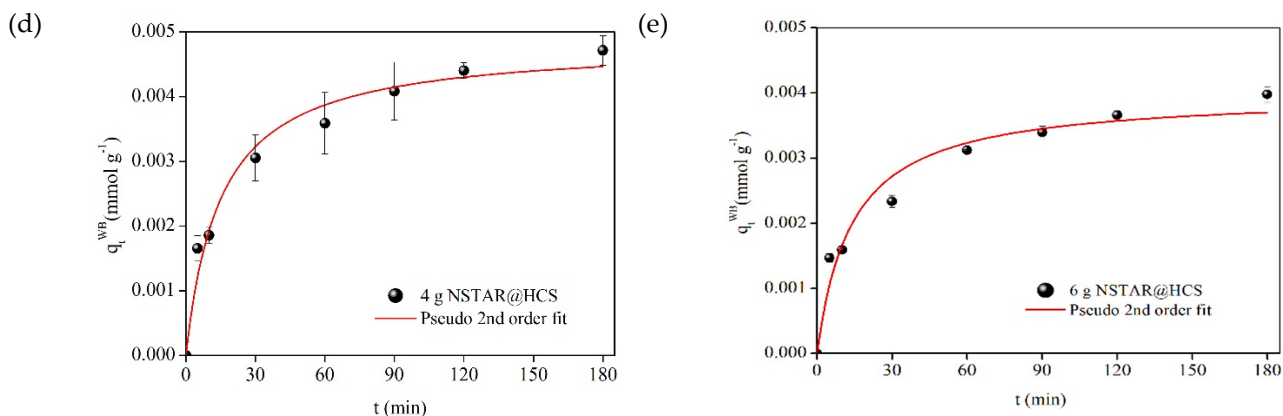


Figure S4. Kinetic adjustments (q_t^{WB}) using 1-6 g NSTAR@HCS in each case. Initial conditions: liquid laboratory waste, $[Cr(VI)]_0=30$ ppm, $pHi=6.5$, $t=180$ min.

For the kinetic data testing different masses of NCs, we chose to show the one with the best fit (higher R^2) of the methods tested. The graphs depicts results up to 180 min, although the experiments were extended to 24 h to determine whether each system had reached equilibrium.

Chromium Removal Capacity in Real Water

Table S2. Cr(VI) and Cr(TOTAL) concentrations obtained after 24 h for different masses of NSTAR@HCS.

M NCs (g)	[Cr(VI)] (ppm)	[Cr(TOTAL)] (ppm)
2	21.24 ± 0.06	21.21 ± 0.36
3	17.18 ± 0.3	18.56 ± 0.47
4	8.56 ± 0.94	8.38 ± 0.44
6	2.14 ± 0.21	1.97 ± 0.24

Cost Analysis and Feasibility of NSTAR@HCS for Cr(VI) Effluent Treatment

Table S3. Costs associated with the electricity consumption required to produce NCs based on nZVI and CS.

Equipe	Potency (W)	Hours of use (h)	Total consumption (KWh)
Magnetic stirrer	36	3	0.108
Syringe pump	5	1	0.005
Ultrasonic washing machine	300	0.25	0.075
Water purification equipment	50	0.5	0.025
Total (for 50 g of NCs)	391	4.75	0.213
Total (for 3.6 Kg of NCs)			15.336
\$/kWh		ARS 83.649	USD 0.088
Electricity cost of synthesis		ARS 1282.84	USD 1.35/h

- I. Rychluk et al. Harnessing chitosan beads as an immobilization matrix for nZVI for the treatment of Cr(VI) contaminated laboratory residue.

References

1. Sheydvasser, A.: 3.1 Steiner's porism and 3.6 Steiner's porism revisited, Linear Fractional Transformations, Undergraduate Texts in Mathematics, Springer International Publishing, pp. 75–81, 99–101, 2023. doi:10.1007/978-3-031-25002-6, ISBN 978-3-031-25001-9